J. Build. Mater. Struct. (2022) 9: 122-132 *Original Article*
DOI : 10.34118/jbms.v9i2.1772

Fatigue behavior of damaged concrete beams repaired with composite material

K. Hadjazi [1,*], A. Hamiani[1], Z. Sereir[1], S. Amziane[2]

1 Laboratoire de Structures de Composites et Matériaux innovants, Faculté de Génie Mécanique, Université des Sciences et de la Technologie d'Oran, BP 1505 El M'naouer, USTO, Oran, Algérie.
2 Université Clermont Auvergne, CNRS, INP Clermont, Institut Pascal, F-63000 Clermont-Ferrand, France.
* Corresponding Author: khamishadj@yahoo.fr

Received: 31-01-2022 **Accepted: 21-08-2022**

Abstract. By the present paper, an analytical model was developed to study the cracked FRP-strengthened reinforced concrete beams subjected to fatigue loading. In order to follow the distribution of interfacial shear stresses causing the debonding phenomenon, a new analytical model based on the cohesive zone (CZ) approach was developed. The present model has the possibility to describe the evolution of the shear stress in the three zones (elastic, microcrack and debonding) and the bearing capacity of the repaired structure. Interface damage scenarios were evaluated for a fatigue load estimated to 90% of the elastic load and another at 60% of the ultimate load *Pu*. Results obtained are in good agreement with those given by the literature. The results showed that the shear strength developed by the repaired beam is sensitive to the variation of the mechanical properties (Concrete, FRP and Adhesive layer), the fatigue load ratio and the number of cycles. These parameters can be considered as indicators of damage affecting the health status of the structure repaired during fatigue. The debonding at the FRP-concrete interface noticeably reduced the strength and lifespan of the repaired structure.

Key words: FRP/concrete, Crack, Repair, Fatigue, CZ model, Shear stresses, Debonding.

1. Introduction

In order to preserve the existing structures and not to resort to the manufacture of new buildings, the recourse to the repair of constructions degraded by their aging, proves to be an effective solution. For this reason, new and innovative methods must therefore be developed, including the technique of rehabilitation of structures by adding bonded composite reinforcements. This technique constitutes a rapid and economical solution for consulting engineers to a growing need for repairing aging or damaged structures. However, and despite the many advantages offered by composite materials (a good resistance in terms of service life of RC structures reinforced under cyclic loading), their adaptations to reinforcement applications reveal many problems, (Wu et al., 2003; Diab et al., 2009). The major problem in this technique is the debonding of the material edge by fatigue or creep loads caused by the sliding between the FRP plate and the concrete beam. This phenomenon creates the great interface shear stresses developed during this loading. In this context, several authors have proposed an analytical method to solve static and dynamic separation problems in FRP reinforced concrete beams (Tounsi, 2006; Wang, 2006; Bennegadi et al., 2016; Houachine et al., 2022). Among the tools most used in the literature to study the fatigue behavior of adhesively bonded joints in structural applications is the cohesive zone model (CZM) approach (Rezazadeh and Carvelli, 2018; Ghovanlou et al., 2014). This model relates the stresses to the displacement through an interface where the crack can be created.

In order to identify the problem of the cracks propagation at the interface, (Hadjazi et al., 2012 and 2016) have developed an analytical model to describe the behavior of the FRP-to-concrete bonded interfaces during the short and long term. (Wahab et al., 2012; Wahab et al., 2015) proposed an analytical model to predict the interfacial stress distribution and the fatigue life of RC beams strengthened with FRP plate under fatigue loads. In recent years, the application of the CZM has been extended to fatigue damage evolution analysis in the repair applications especially at FRP-to-concrete bonded interface. In this purpose, damage parameters are introduced into the CZM to quantify the degradation of the interfacial stiffness and strength under cyclic loading (Xinyan et al., 2019; Johar et al., 2014). (Roe and Siegmund, 2003) used the damage mechanics concept into the CZM and developed a damage evolution model. (Xuan and Vormwald, 2013) proposed a CZM to describe the fatigue damage process. For fatigue models applied to structures reinforced with prestressed FRPs, (Oudah and El-Hacha, 2013) presented a model taking into account the degradation of material properties (concrete and epoxy-concrete) under cyclic loading. (Chen and Cheng, 2016) developed an analytical model to evaluate the shear stresses distribution of the FRP-concrete interface under fatigue load. Based on the above papers, the present study aims to estimate the behavior of cracked FRP-strengthened reinforced concrete beams under cyclic loads. The purpose of this work is to highlight an analytical model that addresses the interface problems between the cracked concrete beam repaired by a composite plate under fatigue load using CZM. The proposed model gives the shear stresses distribution in three zones (elastic, microcrack, debonding zone) near the crack and the bearing capacity of the repaired structure. A fatigue life prediction was also presented to capture the fatigue life of reinforced concrete (RC) structures. Finally, a parametric study was carried out to test the sensitivity of our model to the variation in the number of cycles and load level on the fatigue behavior of FRP-to-concrete interface.

2. CZM for fatigue life prediction of RC beam strengthened with FRP

2.1 Performance degradation of concrete under fatigue loading

Under cyclic loading, the elastic modulus of concrete beam decrease versus the loading cycle number. Due to the internal damage accumulation of concrete, several research (Xinyan et al., 2019; Sherif et al., 2001) showed that the elastic modulus of concrete ($E_{1,N}$) varied continuously under the effect of the fatigue load. This variation is given by:

$$E_{1,N} = \left(1 - 0.33\frac{N}{N_f}\right)E_1 \tag{1}$$

Where, E_1 is the initial Young's modulus of the concrete beam, N is the number of cycles and N_f is the number of accumulated load cycles to concrete failure. In addition, the maximum compressive stress of concrete (σ_{ci}) can be given by (Wu, 2003):

$$\sigma_{ci} = 0.9885 f_c - 0.0618 f_c \lg N_f \tag{2}$$

Where, f_c is the uniaxial compressive strength.

2.2. Performance degradation of FRP plate under fatigue loading

In order to evaluate the fatigue degradation of the FRP plate mechanical properties, (Bigaud and Ali, 2014) proposed a simplified expression to predict the effective elasticity modulus of the FRP plate versus the number of cycles N, as follows:

$$E_2(N) = E_2(1 - 0.071\log_{10}(N)) \tag{3}$$

With, E_2 is the initial Young's modulus of the FRP plate.

2.3. Performance degradation of the interface under fatigue loading

The cumulative damage of FRP-to-concrete interface during the fatigue process is quantified in terms of a damage parameter. The fatigue damage accumulation of the interface was defined by, (Johar et al., 2014):

$$D_{cyc} = 1 - N^{b} \tag{4}$$

From (Johar et al., 2014), the degradation of initial elastic stiffness at the interface, K^N, can be estimated by:

$$K^N = K^{N=0}\left(1 - D_{cyc}\right) \tag{5}$$

Where, $K^{N=0}$ is the interface stiffness during the loading process at $N=0$. b is a constant determined experimentally.

3. Analytical CZM for fatigue behavior

To evaluate the accuracy of the proposed model, a simply supported concrete beam, cracked at mid-span and strengthened by a composite material, was analyzed. The retrofitted beam is made by: concrete, adhesive layer and FRP reinforcement. The concrete beam strengthened by FRP plate is subjected to fatigue three point loads with a flexural pre-crack at mid-span (Figure 1, a).
The geometry of the plated beam is similar to that proposed by (Wang, 2006; and Wang and Zhang, 2008; Hadjazi et al., 2016). The subscripts 1 and 2 denote the concrete beam and the FRP plate, respectively.

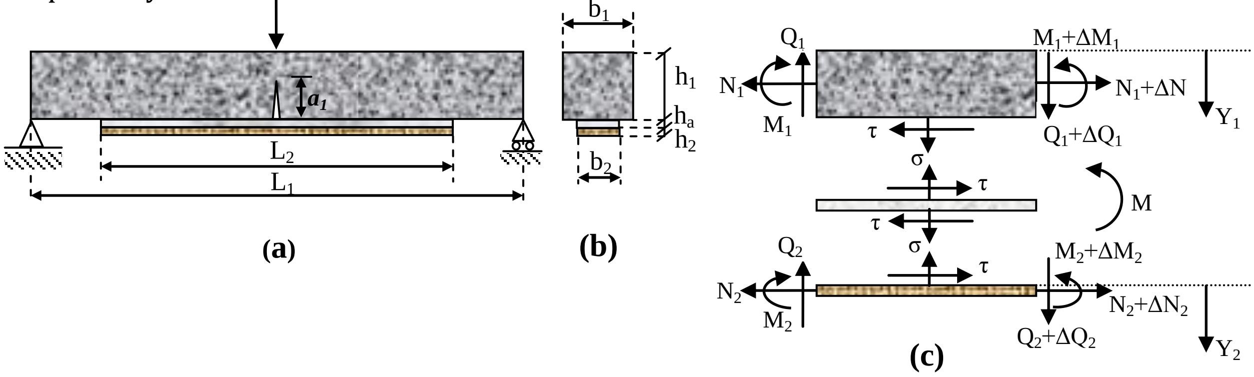

Fig 1. Composite-plate RC beam with a mid-span crack.

Figure 1, c, shows a section of the forces in infinitesimal element of a FRP-plated reinforced concrete (RC) beam. In this Figure Q, N and M are the shear force, the horizontal axial force and couple moment, respectively.
Using elasticity laws, the axial forces N_i and bending moments M_i for these two beams (i = 1, 2) read:

$$N_i = E_{i,N} A_i \frac{du_i}{dx}$$
$$M_i = -E_{i,N} I_i \frac{d^2 w_i}{dx^2} \tag{6}$$

Where u_i and w_i are the axial and vertical displacements of beam i (i = 1, 2), respectively.
$A_i=b_ih_i$, $E_{i,N}$, b_i, h_i and I_i are cross section of beam i, Young's modulus of beam i , width and height of beam i and the moment of inertia of the beam i (i = 1, 2) , respectively
Considering a typical infinitesimal isolated body as shown in Figure 1,c, the equilibrium equations on axial direction and bending moment are given by:

$$\frac{dN_1}{dx} = b_1 \tau \tag{7}$$

$$\frac{dN_2}{dx} = -b_2 \tau \tag{8}$$

$$M = M_1 + M_2 + N_2(Y_1 + Y_2 + h_a) \tag{9}$$

τ is the interface shear stress. Y_1 and Y_2 are the distances from the bottom of adherent 1 and the top of adherent 2 to their centroids respectively.
If the depth of the crack is known, the rotational stiffness of the spring K_r is given as (Paipetis and Dimarogonas, 1986):

$$K_r = c(a_1, h_1)(E_{1,N}\, I_1) \tag{10}$$

Where a_1 is the depth of the crack, For $a_1 < 0.6h_1$, c(a_1, h_1) is given by (Paipetis and Dimarogonas, 1986).

Base on the concept of CZM in static loading, a new concept of the CZM is presented for a fatigue cyclic loading. The analytical model is based on the progressive degradation of CZM parameters of concrete and FRP plate as the number of cycles increased until the debonding initiates and grows along the interface FRP-concrete. For that, a bilinear traction-separation law is supposed for simplicity to adequately describe the cohesive behavior of the adhesive joint interface and the fatigue behavior of RC beam strengthened by FRP. From Figure 2, All CZM parameters are expected to degrade under cyclic loading.

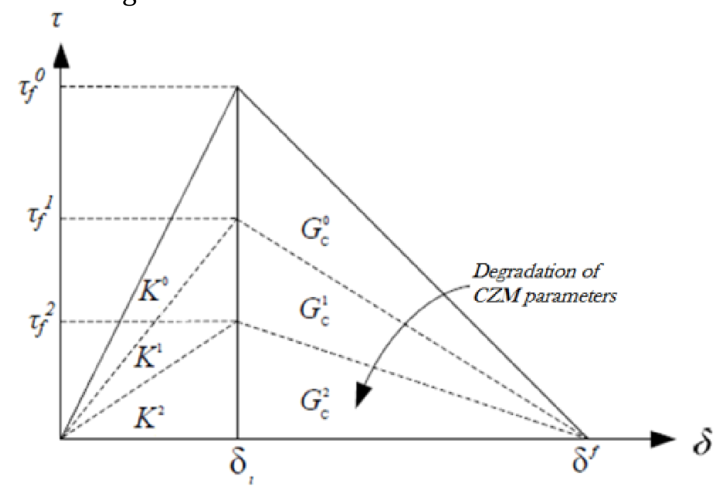

Fig 2. Cyclic degradation of FRP-concrete interface, (Johar et al., 2014).

The use of the CZM (Figure 2) aims to analyze the separation of the interface and to determine the bearing capacity of the beam repaired by a nonlinear method. Therefore, during the loading phase, the nonlinear relationship (Dai et al., 2005; Attari et al., 2010) adopted can be described by the following equations set:

$$\tau = \begin{cases} \dfrac{\tau_f^N}{\delta_1}\delta & 0 \le \delta \le \delta_1 \quad \textit{Elastic Zone} \\ \dfrac{\tau_f^N}{\delta_f - \delta_1}(\delta_f - \delta) & \delta_1 \le \delta \le \delta_f \quad \textit{Softening Zone} \\ 0 & \delta > \delta_f \quad \textit{Debonding Zone} \end{cases} \tag{11}$$

Where, τ_f^N and δ_f are the interfacial bond strength and the separation slip for the fatigue loading.

The separation of the interface δ in the shear directions under cyclic loading is given by (Wang, 2006; Hadjazi et al., 2012):

$$\delta = u_1 - Y_1 \frac{\partial w_1}{\partial x} - u_2 - Y_2 \frac{\partial w_2}{\partial x} \tag{12}$$

As the number of cycles increased, the slip along the interface δ, become:

$$\delta = \delta^N + \delta^{N+1} \tag{13}$$

Where δ^N and δ^{N+1} are the slip along the interface under fatigue loading at *N* and *N+1* cycle, respectively.

The area under the traction-relative displacement curve is the fracture energy G_c^N written as:

$$G_c^N = \frac{1}{2}\tau_f^N \delta_f \tag{14}$$

Using the CZM, the fatigue behavior of concrete beams reinforced by FRP plate for these three stages is given as follows.

3.1. Elastic zone

In this zone, the distribution of interfacial shear stresses is given by substituting Eq. (12) into the first equation of Eq. (11).

$$\frac{\partial \tau}{\partial x} = \frac{\tau_f^N}{\delta_1}\left(\frac{\partial u_1}{\partial x} - Y_1\frac{\partial^2 w_1}{\partial x^2} - \frac{\partial u_2}{\partial x} - Y_2\frac{\partial^2 w_2}{\partial x^2}\right) \tag{15}$$

Substituting Eq. (6) into Eq. (15), we have:

$$\frac{d\tau}{dx} = \frac{\tau_f^N}{\delta_1}\left(\frac{N_1}{E_{1,N}A_1} - \frac{N_2}{E_{2,N}A_2} - Y_1\frac{d^2 w_1}{dx^2} - Y_2\frac{d^2 w_2}{dx^2}\right) \tag{16}$$

According to the literature (Hadjazi et al., 2012; Rasheed and Pervaiz, 2002), the FRP plate and the concrete beam have the same curvature, i.e.

$$\frac{\partial^2 w_1}{\partial x^2} = \frac{\partial^2 w_2}{\partial x^2} \tag{17}$$

Substituting Eq. (17) and Eq. (6) into Eq. (9), Eq. (16) becomes:

$$\frac{d\tau}{dx} = \frac{\tau_f^N}{\delta_1}\left(\frac{N_1}{E_{1,N}A_1} - \frac{N_2}{E_{2,N}A_2} - \frac{Y_1+Y_2}{E_{1,N}I_1+E_{2,N}I_2}\left(-M + \left(Y_1+Y_2+h_a\right)N_2\right)\right) \tag{18}$$

Differentiating both sides of Eq. (18) and considering equilibrium Eqs. (7)–(8) we obtain:

$$\frac{d^2\tau}{dx^2} = K^N\left(\frac{1}{E_{1,N}A_1} + \frac{1}{E_{2,N}A_2} + \frac{\left(Y_1+Y_2\right)(Y_1+Y_2+h_a)}{E_{1,N}I_1+E_{2,N}I_2}\right)b_2\tau + K^N\left(\frac{Y_1+Y_2}{E_{1,N}I_1+E_{2,N}I_2}\right)M' \tag{19}$$

With: $N_1 = -N_2$ and $K^N = \tau_f^N / \delta_1$

The differential equation of the second order (19) takes the solution:

$$\tau = Ae^{-\lambda_1 x} + Be^{\lambda_1 x} + \tau_c \tag{20}$$

τ_c: is the particular solution, where:

$$\lambda_1 = C_\lambda\sqrt{K^N}$$

$$\tau_c = C_\tau M'$$

$$C_\lambda = \sqrt{b_2\left(\frac{1}{E_{1,N}A_1} + \frac{1}{E_{2,N}A_2} + \frac{(Y_1+Y_2+h_a)(Y_1+Y_2)}{E_{1,N}I_1+E_{2,N}I_2}\right)} \tag{21}$$

$$C_\tau = \frac{Y_1 + Y_2}{\left(E_{1,N} I_1 + E_{2,N} I_2\right) C_\lambda^{\ 2}}$$

When x is sufficient large, shear stress is limited and converges to its particular solution τ_c so $B=0$, (Wang and Qiao, 2004). To determine the value of A, displacement boundary condition at $x = 0$ is used. The corresponding slip δ along the interface in elastic stage can be easily obtained by substituting Eq. (20) into the first equation of Eq. (11).

$$\delta^N = \frac{\delta_1}{\tau_f^N}\left(Ae^{-\lambda_1 x} + \tau_C\right) \tag{22}$$

3.2. Elastic-Microcrack zone

For loading and unloading conditions, the substrates deform. A part of the interface begins to soften and two regions along the interface are formed:

a) In the linearly elastic region *($\delta_N \leq \delta_1$)*, the solution of shear stress has the same form as in Eq. (20) with the same condition of $B_1 = 0$.

$$\tau = A_1 e^{-\lambda_1 (x - a_1)} + \tau_c \tag{23}$$

The coefficient A_1 is obtained by the following boundary condition at $x = a_1$. From the Eq. 11 and Eq. (23), the slip δ along the interface for this region is given by:

$$\delta = \frac{\delta_1}{\tau_f^N}\left(A_1 e^{-\lambda_1 (x - a_1)} + \tau_c\right) \tag{24}$$

Where a_1 is the length of the microcrack zone. The coefficient A_1 is obtained by the following boundary condition at $x = a_1$:

$$\tau\big|_{x=a_1} = \tau_f^N \tag{25}$$

b) In the microcrack zone *($\delta_1 \leq \delta_N \leq \delta_f$)*, the second bond-slip relation expression of Eq. (11) and Eqs. (6), (12) and (17) becomes:

$$\frac{d^2\tau}{dx^2} = -K_2^N\left(\frac{1}{E_{1,N}A_1} + \frac{1}{E_{2,N}A_2} + \frac{\left(Y_1 + Y_2\right)}{E_{1,N}I_1 + E_{2,N}I_2}\left(Y_1 + Y_2 + h_a\right)\right) b_2 \tau - K_2^N\left(\frac{Y_1 + Y_2}{E_{1,N}I_1 + E_{2,N}I_2}\right) M' \tag{26}$$

With: $K_2^N = \dfrac{\tau_f^N}{\delta_f - \delta_1}$

The differential equation of the second order (26) takes the solution:

$$\tau = C\cos(\lambda_2 (x - a_1)) + D\sin(\lambda_2 (x - a_1)) + \tau_C \tag{27}$$

From Eqs. (11) and (27), the corresponding slip δ along the interface for this region is given by :

$$\delta = \delta_f - \frac{\delta_f - \delta_1}{\tau_f}\left(C\cos(\lambda_2 (x - a_1)) + D\sin(\lambda_2 (x - a_1)) + \tau_C\right) \tag{28}$$

Where:

$$\lambda_2 = C_\lambda \sqrt{K_2^N} \tag{29}$$

The coefficients C and D are determined by continuous conditions at $x = a_1$.

As the number of cycles increased, the material is damaged gradually until the debonding at the FRP-concrete interface.

3.3. Elastic, microcrack and debonding zone

In this section the three stages, elastic, microcrack and debonding zone are considered. The shear stress for each stage is given by:

- Elastic zone: $$\tau = A_1 e^{-\lambda_1 (x-d-a_u)} + \tau_c \tag{30}$$
- Microcrack zone: $$\tau = C\cos(\lambda_2 (x-d-a_u)) + D\sin(\lambda_2 (x-d-a_u)) + \tau_C \tag{31}$$
- Debonding zone: $$\tau = 0 \tag{32}$$

4. Results and discussion

In the present section, results are presented and discussed in terms of stress distribution in the interface, progressive interface damage accumulation and bearing capacity of repaired structure.
For all applications, mechanical and geometrical characteristics given in Tables 1 and 2 are the same as those used by (Hadjazi et al., 2016; Wu, 2003).

Table1: Mechanical properties of FRP plate-concrete for N=0.

E_1 [GPa]	E_2 [GPa]	$\tau_f^{N=0}$ [MPa]	$K^{N=0}$ [MPa/mm]	$G_f^{N=0}$ [N/mm]	f_c [MPa]
25	230	1.8	160	0.5	20-80

Table2: Geometrical properties of FRP plate-concrete.

L [mm]	L_1 [mm]	h_1 [mm]	h_2 [mm]	h_a [mm]	b_1 [mm]	b_2 [mm]	b_a [mm]	$c(a_1, h_1)$
750	700	150	0.11	0.1	100	100	100	0.0001167

The FRP-strengthened reinforced concrete beams was subjected to repeated fatigue loading, with constant amplitude. Figure 3 shows the cyclic loading with a positive stress ratio.

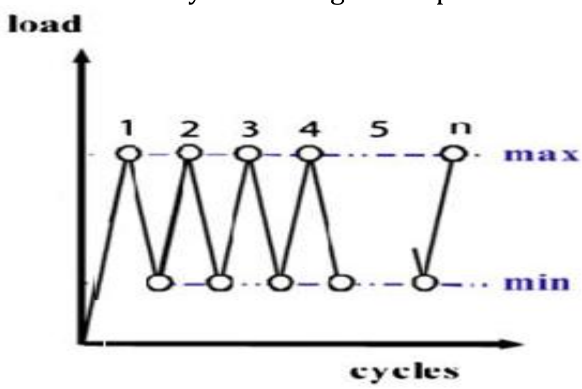

Fig 3. Loading and unloading condition

To provide the fatigue resistance of the repaired concrete beam, the evolution of shear stress at the adhesive interface throughout the applied fatigue cycles is illustrated in Figure 4. Under fatigue loading, the evolution of shear stress is caused by both degradation of concrete beam and the FRP plate. Near the flexural crack tip, the increase of fatigue cycles has a significant effect on shear stress evolution, particularly at the microcrack zone until full debonding initiates (at $N \approx 10^6$ cycles). We deduced that, the increase in the fatigue cycles affect significantly the distribution of shear stress along the interface between FRP and concrete and debonding growth.

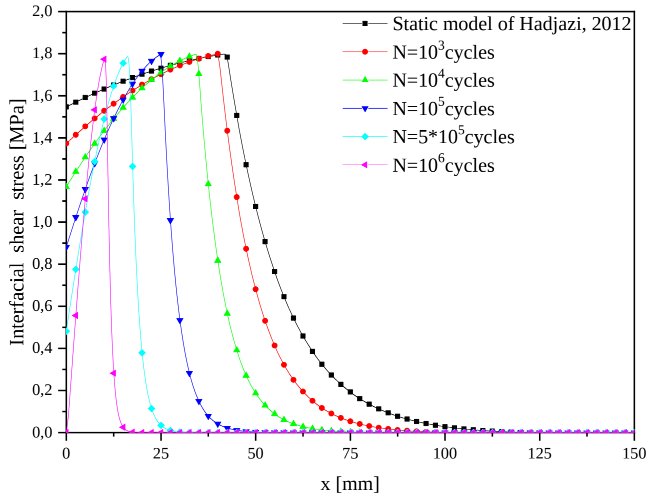

Fig 4. Fatigue load-interfacial shear stress.

Figure 5, examines the effect of cycles number (at failure) on the externally applied load evolution against the bond slip. It is clearly visible that an increase in the number of cycles generates a reduction in the fatigue capacity of the FRP-concrete bond. This reduction is caused by the degradation of the mechanical performance of the concrete/FRP plate. For fatigue loads close 24% of the ultimate static capacity, FRP reinforced concrete beams often yield to 10^6 cycles. So, it is possible to predict the fatigue life of our repaired structure depending on the load level.

Both Figures 6 and 7 represent the bond slip curves of FRP-plate concrete beam for two load ratios ($R = P_{min}/P_{max}$). The R lower limit was set to 60% of *Pe* and 30% of *Pu*, (R=0.5). But, the R upper limit was set to 90% of *Pe* and 60% of *Pu* of the static bond capacity (R=0.66). Where *Pe* is the maximum value of static load applied to the beam without causing softening in the FRP-concrete interface and *Pu* is the ultimate static load (Hadjazi et al., 2012), respectively. From both Figures, we noticed that the variation of R changes remarkably the fatigue behavior of FRP-concrete interface.

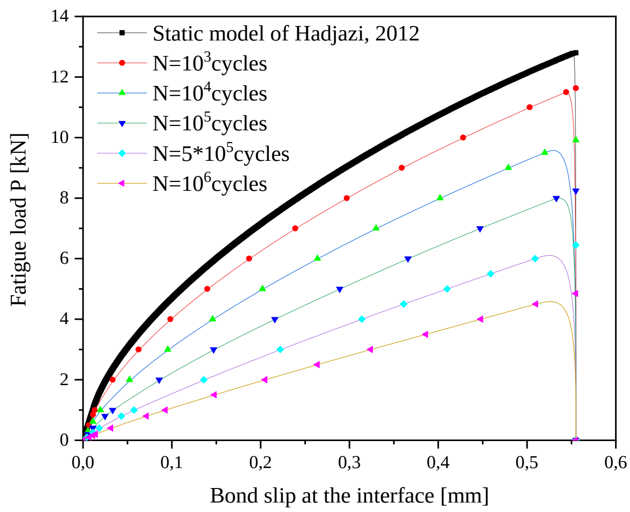

Fig 5. Fatigue response of interfacial bond slip.

After a series of N cycles (Figure 6), the bond slip at the interface is not reached because the interface still remains in the elastic zone. From Figure 7, interface damage progression can be separated into three stages; cracks initiation, damage accumulation and debonding stage. This damage development results from the degradation of the strength and the rigidity of the interface CFRP-concrete (3,5 10^4 cycles). In this regard, cyclic loading and R have the significant effects on the bond between FRP materials and concrete. This causes a reduction in bond strength and an acceleration of bond deterioration as the cycle number increases.

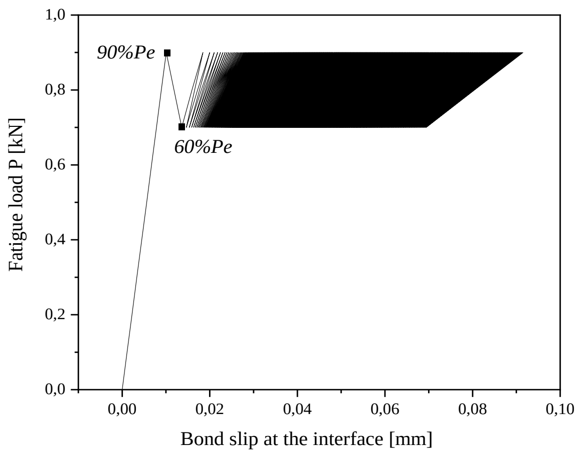

Fig 6. Fatigue response of interfacial bond slip for a loading ratio R = 0.66

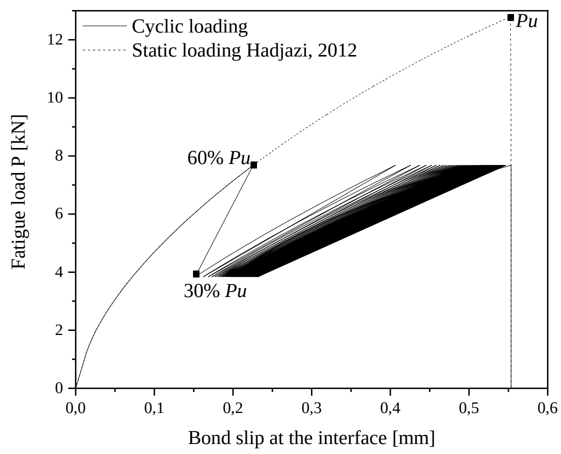

Fig 7. Fatigue response of interfacial bond slip for a loading ratio R = 0.5

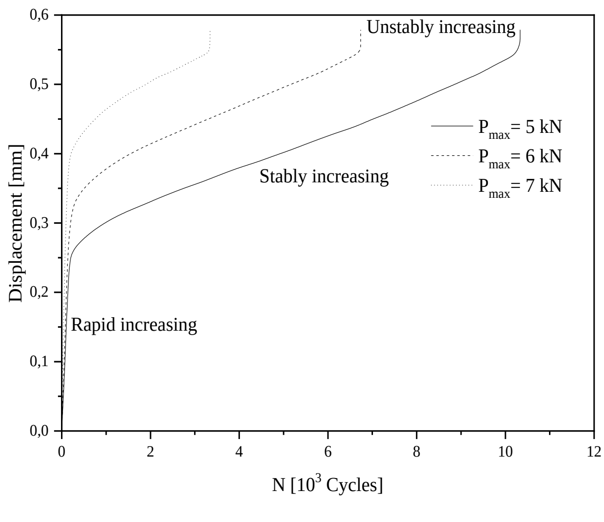

Fig 8. Curves of displacement-cycles under different loading level

The relationships between the displacement (slip) and the number of loading cycles for cracked FRP-strengthened reinforced concrete beams with different loading levels are presented in Figure 8. From this Figure, it's clearly visible that the fatigue behavior of the interface can be divided into three stages: the fast propagation, the stable propagation and the unstable propagation stage. In all three stages, the initiation and rupture time is very short. The stable propagation stage accounts for approximately 95% of the total fatigue life. It can also be seen that a higher load level causes greater damage. Moreover, the service life of the retrofitted beam decreases with increasing loading level.

5. Conclusion

An analytical model based on the cohesive zone approach has been developed to predict the fatigue life of FRP strengthened RC beam. The model considers the degradation of the concrete, interface and FRP plate. This study predicted the fatigue life, interfacial shear stresses distribution, and load-bearing capacity of FRP-repaired reinforced concrete beams. Based on the results, the following conclusions were drawn:

- The model is able to capture the evolution of interfacial shear stresses with increasing load cycles, and the number of load cycles to failure.
- The cumulative damage of the interface increases with the number of loading cycles.
- The cumulative damage growth rate of the interface became important with the increase of load level.
- The service life and the bearing capacity of cracked FRP-strengthened reinforced concrete beams decreases as the cyclic loading and load frequency increases. This decrease takes place due to the losses in the resistance and rigidity of the component materials.

Acknowledgments

The author would like to acknowledge Prof. SEREIR Zouaoui, director of the Laboratory for Structures of Composites and Innovative Materials and all members of the laboratory for their contribution.

6. References

Attari, N., Amziane, S., & Chemrouk, M. (2010). Efficiency of beam–column joint strengthened by FRP laminates. Advanced Composite Materials, 19(2), 171-183.

Bennegadi, M. L., Hadjazi, K., Sereir, Z., Amziane, S., & El Mahi, B. (2016). General cohesive zone model for prediction of interfacial stresses induced by intermediate flexural crack of FRP-plated RC beams. Engineering Structures, 126, 147-157.

Bigaud, D., & Ali, O. (2014). Time-variant flexural reliability of RC beams with externally bonded CFRP under combined fatigue-corrosion actions. Reliability Engineering & System Safety, 131, 257-270.

Chen, C., & Cheng, L. (2016). Theoretical solution to fatigue bond stress distribution of NSM FRP reinforcement in concrete. Composites Part B: Engineering, 99, 453-464.

Dai, J., Ueda, T., & Sato, Y. (2005). Development of the nonlinear bond stress-slip model of fiber reinforced plastics sheet-concrete interfaces with a simple method. Journal of composites for construction, 9(1), 52-62.

Diab, H. M., Wu, Z., & Iwashita, K. (2009). Theoretical solution for fatigue debonding growth and fatigue life prediction of FRP-concrete interfaces. Advances in structural engineering, 12(6), 781-792.

Ghovanlou, M K., Jahed, H., & Khajepour, A. (2014). Cohesive zone modeling of fatigue crack growth in brazed joints. Engineering Fracture Mechanics, 120, 43-59.

Hadjazi, K., Sereir, Z., & Amziane, S. (2012). Cohesive zone model for the prediction of interfacial shear stresses in a composite-plate RC beam with an intermediate flexural crack. Composite Structures, 94(12), 3574-3582.

Hadjazi, K., Sereir, Z., & Amziane, S. (2016). Creep response of intermediate flexural cracking behavior of reinforced concrete beam strengthened with an externally bonded FRP plate. International journal of solids and structures, 94, 196-205.

Houachine, H. R., Sereir, Z., & Amziane, S. (2022). Creep model for the long-term behaviour of combined cohesive-bridging model of FRP–concrete interface debonding under axial loading. European Journal of Environmental and Civil Engineering, 26(12), 5594-5616.

Johar, M., Kosnan, M. S. E., & Tamin, M. N. (2014). Cyclic cohesive zone model for simulation of fatigue failure process in adhesive joints. In Applied Mechanics and Materials (Vol. 606, pp. 217-221). Trans Tech Publications Ltd.

Oudah, F., & El-Hacha, R. (2013). Analytical fatigue prediction model of RC beams strengthened in flexure using prestressed FRP reinforcement. Engineering Structures, 46, 173-183.

Paipetis, A. S., Dimarogonas, A. D. (1986). Analytical Methods in Rotor Dynamics. Elsevier Applied Science, London.

Rasheed, H. A., & Pervaiz, S. (2002). Bond slip analysis of fiber-reinforced polymer-strengthened beams. Journal of engineering mechanics, 128(1), 78-86.

Rezazadeh, M., & Carvelli, V. (2018). A damage model for high-cycle fatigue behavior of bond between FRP bar and concrete. International Journal of Fatigue, 111, 101-111.

Roe, K. L., & Siegmund, T. (2003). An irreversible cohesive zone model for interface fatigue crack growth simulation. Engineering fracture mechanics, 70(2), 209-232.

Sherif El-Tawil, Ogunc, C., Okeil, A., & Shahawy, M. (2001). Static and fatigue analyses of RC beams strengthened with CFRP laminates. Journal of composites for construction, 5(4), 258-267.

Tounsi, A. (2006). Improved theoretical solution for interfacial stresses in concrete beams strengthened with FRP plate. International Journal of solids and Structures, 43(14-15), 4154-4174.

Wahab, N., Soudki, K. A., & Topper, T. (2012). Experimental investigation of bond fatigue behavior of concrete beams strengthened with NSM prestressed CFRP rods. Journal of composites for construction, 16(6), 684-692.

Wahab, N., Topper, T., & Soudki, K. A. (2015). Modelling experimental bond fatigue failures of concrete beams strengthened with NSM CFRP rods. Composites Part B: Engineering, 70, 113-121.

Wang, J. (2006). Cohesive zone model of intermediate crack-induced debonding of FRP-plated concrete beam. International journal of solids and structures, 43(21), 6630-6648.

Wang, J., & Qiao, P. (2004). Interface crack between two shear deformable elastic layers. Journal of the Mechanics and Physics of Solids, 52(4), 891-905.

Wang, J., & Zhang, C. (2008). Nonlinear fracture mechanics of flexural–shear crack induced debonding of FRP strengthened concrete beams. International journal of solids and structures, 45(10), 2916-2936.

Wu, Z., & Yin, J. (2003). Fracturing behaviors of FRP-strengthened concrete structures. Engineering Fracture Mechanics, 70(10), 1339-1355.

Wu, Z., Iwashita, K., Ishikawa, T., Hayashi, K., Hanamori, N., Higuchi, T., ... & Ichiryu, T. (2003). Fatigue performance of RC beams strengthened with externally prestressed PBO fiber sheets. In Fibre-Reinforced Polymer Reinforcement for Concrete Structures: (In 2 Volumes) (pp. 885-894).

Xinyan, G., Wang, Y., Huang, P., & Chen, Z. (2019). Finite element modeling for fatigue life prediction of RC beam strengthened with prestressed CFRP based on failure modes. Composite Structures, 226, 111289.

Xuan, C., & Vormwald, M. (2013). Application of a new cohesive zone model in low cycle fatigue. Solids and Structures, 2(3), 31-40..